Indian J Phys (February 2019) 93(2):147–158
https://doi.org/10.1007/s12648-018-1280-7

ORIGINAL PAPER

Conductivity and free volume studies on bismuth sulfide/ PVA:polypyrrole nanocomposites

V Hebbar[1], H B Ravikumar[2], M Nandimath[1], S Masti[3], L M Munirathnamma[2], J Naik[4] and R F Bhajantri[1]*

[1]Department of Physics, Karnatak University, Dharwad, Karnataka 580 003, India

[2]Department of Studies in Physics, University of Mysore, Manasagangotri, Mysore, Karnataka 570 006, India

[3]Department of Chemistry, Karnatak Science College, Dharwad, Karnataka 580 001, India

[4]Department of Physics, Mangalore University, Mangalagangotri, Mangalore, Karnataka 574 199, India

Received: 30 January 2018 / Accepted: 22 May 2018 / Published online: 22 August 2018

Abstract: The polymer composite films of polyvinylalcohol:polypyrrole blend containing different wt% of bismuth sulfide (Bi_2S_3) particles are prepared through in situ oxidation followed by solution casting method, where the particles are coated with blend matrix. The XRD studies affirm the enhanced crystallinity of the composites. The variation of crystallite size is measured with the Debye–Scherrer method. The DSC studies are used to investigate the glass transition that occurred in the Bi_2S_3 particles-filled polymer blend matrix. The AFM and SEM studies illustrated the effect of insertion of metallic sulfide particles on the surface morphology. The addition of bismuth sulfide particles results in the increased mechanical properties of the composite matrix. The electrical conductivity is determined by the Cole–Cole plot fitted using equivalent circuit model, and the conductivity is observed to be enhanced with an increase in filler content due to the enhanced conductive pathways. The variation of o-Ps lifetime, o-Ps intensity, average size of the free volume and fraction of free volume is studied using Tao–Eldrup Model. The obtained free volume parameters are correlated with the electrical, microstructural and thermal properties. The increased interfacial width is illustrated in terms of increased free volume size. The enhanced free volume provides more space for mobility of charge carriers, and hence the conductivity is enhanced.

Keywords: Blend; AFM; Mechanical properties; Conductivity; Cole–Cole; Free volume

PACS Nos.: 61.10.Nz; 66.10.Ed; 71.20.Rv; 71.60.+z; 72.80.Le; 78.70.Bj

1. Introduction

Polymer matrix embedded with inorganic particles such as ceramics or metal compounds has attracted the attention of researchers, because of its ease of processing and flexibility for various potential applications such as capacitors, actuators, sensors and printed circuit boards [1]. In recent years, conducting polymer-based composites embedded with metal nanoparticles are of special interest due to their unique electrical properties and potential applications [2]. The polymer blending is used to extract the prominent properties of the component polymers by limiting the drawbacks, and resulting in the novel material with high benefits [3]. In the polymer blend composite materials made up of the components such as basic polymer matrix, conducting polymer and metal derivative particles, the conductivity of the material is enhanced either due to the conducting polymer or due to both the conducting polymer and filler metal particles, while the basic polymer matrix provides the mechanical stability.

In recent years, PPy has been extensively investigated due to its high electrical conductivity, good environmental and thermal stabilities, and the ease of synthesis. In the recent years, the pyrrole-based materials possess a wide range of applications in supercapacitors, solar cells, energy storage devices and bio-sensors, etc. [4]. However, the mass production of PPy is restricted because of its brittleness and poor mechanical strength. The mixing of the conducting polymers with natural polymers or thermoplastic polymers yields a composite material with good

*Corresponding author, E-mail: rfbhajantri@gmail.com

electrical, mechanical and optical properties. The composites of PPy with excellent stability and flexibility can be prepared by various methods such as vapor polymerization, electrochemical polymerization and chemical polymerization. Among these, chemical polymerization is the widely used method to develop many conductive PPy composites such as PPy/PVA, PPy/PVC [5]. Bi_2S_3 is a member of V-VI group of semiconductors whose energy gap lies in the visible solar energy spectrum, and it has application in optics, magnetic, thermoelectric devices and photovoltaics. The metal sulfide such as Bi_2S_3 generally stores metal ion like sodium by conversion reaction mechanism to the lithium counterpart, and it is also used as anode material in sodium ion batteries [6]. The attempts had been made in the synthesis of 1-D Bi_2S_3 in the free state like powder and also its composites with the polymers such as PVA, PEDOT, PANI, PVDF [1, 7–9].

Positron annihilation spectroscopy (PAS) is the novel method for the investigation of the interfacial defects due to its high sensitivity to the defect-related phenomena. The ability of thermalized positrons to diffuse and annihilate at the surfaces of grains [10] provide unique molecular level information about the complex macromolecular structure. Positron annihilation lifetime spectroscopy (PALS) is able to give information about the size and number of free volume holes at the nanoscale [11]. These free volume properties are affected by the type and amount of filler in polymer nanocomposites.

When positrons from ^{22}Na radioactive source are injected into the condensed medium like polymers, they get thermalized (slowed down) by losing their energy through inelastic collisions. Such a positron can annihilate either directly with the electrons as quasi-free positron known as 'free annihilation' or indirectly by forming a bound state with the electron in the medium called 'positronium'(Ps) or can form a localized state named as 'trapped annihilation' [12, 13]. A positronium' (Ps) is a hydrogen-like bound state, which can form in two ways: para-positronium (p-Ps) which exists in the form of singlet spin state (particles of anti-parallel spin) and ortho-positronium (o-Ps) which exists in the form of triplet spin state (particles of parallel spin). The intrinsic lifetime of p-Ps is 125 ps in a vacuum and is much lesser than that of o-Ps i.e., 142 ns [11]. In polymers, o-Ps are preferentially localized in the free volume cavity and annihilate with the electron possessing an anti-parallel spin present in the surrounding medium known as 'pick-off annihilation'. This reduces the o-Ps lifetime by few nanoseconds and results in the emission of two gamma rays. The components of the PALS spectra give the information about all these types of annihilations. The short-lived component (τ_1) and intermediate lifetime (τ_2) are able to give the information about self-annihilation of p-Ps, free annihilation and trapped annihilation, respectively. The longest component (τ_3) corresponding to the pick-off annihilation of o-Ps is the key parameter to estimate the free volume-related properties of the polymeric system. The free volumes in a polymer nanocomposite are formed by the irregular arrangement of the polymer chains in the amorphous phase, molecular relaxations of chains or evolution of interfaces between the polymer matrix and filler particles. The open space between the surface of the particles and the innermost polymer layers, which surrounds the particle, can act as the most stable state known as 'interface' [10]. The formation of the interface layer and probable internal structure of the nanoparticle-embedded polymer matrix is represented in Fig. 1. The annihilation of o-Ps can occur in free volumes available in interfaces as well as in matrix [13].

Few results were reported so far on the preparation and study of PVA:PPy polymer blend and as well as their nanocomposites. Ramesan had reported the synthesis of CuS/PPy/PVA composite and mentioned that the nanoparticles-filled composites have shown more DC conductivity than pure PPy [2]. Basavaraja et al. reported the enhanced electrical conductivity and microwave absorption properties of PPy/PVA/graphite oxide nanocomposites [14]. de Melo et al. synthesized PVA/PPy–ZnO fibers and studied their optical mainly fluorescence properties and also I–V characteristics under UV light [4]. However, there were no reports relating the free volume properties with the electrical properties of PVA:PPy blend. There are some reports on the free volume studies of the polymer nanocomposites using PALS. Xue et al. reported the correlation of thermal conductivity with the properties of free volume defects and the interfacial interactions in RGO/PVA composites [13]. Sheela et al. reported the correlation between the enhanced DC conductivity in $LiClO_4$-doped PVA/NaAlg polymer composites with the free volume parameters using PALS [15].

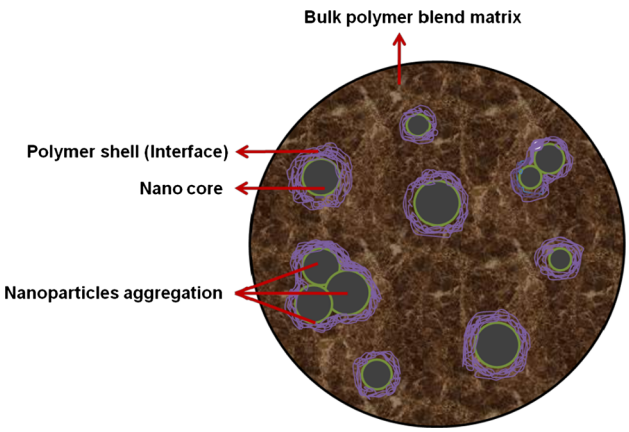

Fig. 1 The probable internal structure of the nanoparticle-embedded polymer matrix

With the prior background, an attempt is made in this work to find the relation of mechanical and conducting properties with the microstructural and free volume in Bi_2S_3 particles (different wt%)-filled PVA:PPy blend composites. With this objective, the PVA:PPy polymer blend composites embedded with different wt% of Bi_2S_3 particles were synthesized by in situ chemical oxidative polymerization. The microstructural variations have been studied by the analysis of X-ray diffraction patterns and AFM images. The thermal response of the composites has been studied using DSC thermograms. The mechanical and conducting properties have been investigated by studying the stress–strain relation and Cole–Cole plot, respectively. The measurement of the free volume properties had been done by using PALS technique.

2. Experimental details

2.1. Materials

The pyrrole monomer (C_4H_5N) with the molecular weight of 67.09 g mol^{-1} procured from Spectrochem Pvt. Ltd. Mumbai, India, was stored at < 5 °C before used for the synthesis. The polymer PVA ($[(-C_2H_4O-)_n]$, M. W. $\sim$ 1,25,000 g mol^{-1}) and $FeCl_3$ (M. W. = 169.21 g mol^{-1}) were purchased from M/s. s. d. fine chemical limited, Mumbai, India. The other reagents such as bismuth nitrate pentahydrate (98% ($Bi(NO_3)_3.5H_2O$, M. W. = 485.07 g mol^{-1}, Alfa Aesar, England), sodium sulfide ($Na_2S{\cdot}9H_2O$) were used in the preparation of the samples as received.

2.2. Samples preparation

2.2.1. Preparation of Bi_2S_3 nanoparticles

The Bi_2S_3 particles were synthesized by using the chemical method at room temperature. In the procedure, $Bi(NO_3)_3.5H_2O$ was dispersed in distilled water (0.01 M) with continuous stirring up to 3 h. The solution of $Na_2S.9H_2O$ (0.03 M) was added drop by drop to this solution until the color changes to dark brown and the mixture was left for 12 h to stabilize [7]. The dark brown precipitate was washed several times with absolute ethanol and distilled water to remove unreacted contents and dried.

2.2.2. Preparation of Bi_2S_3-filled PVA:PPy blend composites

The pure PVA:PPy blend is obtained by dissolving pre-weighed quantity (1.5 g) of the polymer PVA in distilled water (30 ml) by heating at a temperature 40 °C with continuous stirring, and the solution was left to cool down to the room temperature. Then, 0.5 ml of cooled pyrrole monomer is added to the viscous solution of PVA and stirred up to 30 min until it became homogeneous. The above mixture is kept in an ice bath to maintain the temperature 0–5 °C. 2.187 g of $FeCl_3$ is dissolved in 5 ml of distilled water and is added dropwise to the PVA:pyrrole mixture with uniform stirring. The black homogeneous mixture was poured into the glass Petri dishes which were kept in hot air oven at a constant temperature of 30 °C to get the composite films. Bi_2S_3-filled PVA:PPy blend composite films were prepared by the same method. However, in this process, the addition of various wt% (1 wt%, 3 wt%, 5 wt%, 8 wt%) of Bi_2S_3 particles followed by the polymerization of pyrrole in PVA medium by the above-mentioned procedure. The prepared composite films were peeled off after complete drying and stored in vacuum desiccators for the further investigation.

2.3. Samples characterization

The thickness of the peeled dry polymer films was measured using Mitutoyo-7327 dial thickness gauge, which was found to be in the range of 320–340 μm ($\pm$ 1 μm). The powder X-ray diffraction patterns of the samples were recorded using Rigaku Miniflex-600 Benchtop X-ray diffractometer with Cu-K_α radiation of wavelength 1.5406 Å in an angle 2θ range from 5° to 60° with the step size of 0.02° and at a scanning speed of 1°min^{-1}. DSC thermograms were obtained using TA Instruments model DSC Q20 V24.10 Build 122 from 40 to 300 °C with heating at a rate 10 °C min^{-1} in sealed aluminum pans under a nitrogen atmosphere. The weight of the dry sample used for the study is 1–2 mg. The topographical images were recorded using NANOSURF EZ2-FlexAFM in the air at an ambient condition in the dynamic force mode of the tip scanned over an approximate area 1 μm $\times$ 1 μm. The SEM images of pure PVA:PPy blend, 3 and 5 wt% Bi_2S_3-filled PVA:PPy films were recorded using CARL ZEISS instrument with an acceleration voltage of 5 kV, and the scanning was done with WD about 4.7 mm in FEI mode. The mechanical properties of the prepared composite films were studied in terms of tensile strength and percentage elongation measurements. The measurements of mechanical parameters at ambient temperature for the composite films of dimension 60 mm $\times$ 25 mm with 50 mm gauge length were taken using the instrument Dak System Inc series: 7200 with a load of 1 kN. To record the impedance response, the prepared polymer electrolyte film cut into small disks of 1.5 cm diameter was placed between stainless steel blocking electrodes of diameter 1.3 cm. The electrical impedance spectra of the polymer blend nanocomposites were recorded with HIOKI-IM 3570 high

precision impedance analyzer in the frequency range of 4 Hz–5 MHz in analyzer mode.

2.3.1. *Positron annihilation lifetime spectroscopy (PALS)*

The positron lifetime measurements were taken at room temperature by a conventional fast–fast coincidence lifetime spectrometer with a time resolution of 230 ps. The PALS system equipped with a pair of conically shaped BaF_2 scintillators coupled to photomultiplier tubes of type XP2020/Q with quartz window as detectors. On each side, three samples of 2 cm × 2 cm were stacked together to get the required minimum thickness of 1 mm. Such stacked samples were placed on either side of a ^{22}Na positron source with 10 μCi strength, deposited on a pure Kapton foil of 0.0127 mm thickness. The lifetime spectrum is acquired by placing the sandwich of source and sample between the two detectors. Two to three positron lifetime spectra, each with more than a million counts, were acquired in a period of 4–6 h. Consistently, reproducible spectra were analyzed and resolved into three lifetime components with the help of computer program PATFIT-88 with proper source and background corrections. The source correction term and resolution function were estimated from the lifetime of well-annealed aluminum using the program RESOLUTION [16]. The three Gaussian resolution functions were used in the analysis of positron lifetime spectra of the prepared composites.

3. Results and discussion

3.1. X-ray diffraction studies

The XRD patterns of pure PVA:PPy blend, Bi_2S_3-filled PVA:PPy composites and prepared Bi_2S_3 particles are presented in Fig. 2. The pure PVA:PPy blend exhibits an amorphous halo; however, all the Bi_2S_3-filled composites possess the crystalline peaks. A broad peak that appeared at about $2\theta = 20°–40°$ and a small halo near $2\theta = 17.5°$ are characteristics of PVA:PPy [2, 17]. All diffraction peaks exhibited by the pure Bi_2S_3 and Bi_2S_3 particles-filled composites were consistent with the literature data of Bi_2S_3 [18]. The intensity of the characteristic peaks corresponding to Bi_2S_3 in the composites was increased with an increase in wt% up to 3 wt% filling suggest the increased crystallinity of the composites due to ordering of polymer chains at the surface of filler particles by the interfacial interaction [16, 19, 20]. The characteristic amorphous halo of the PVA:PPy blend is depressed after the addition of more amount of Bi_2S_3 particles. The characteristic peaks of Bi_2S_3 had shown very slight shift, which indicates that the lattice structure of Bi_2S_3 does not affect by PVA:PPy

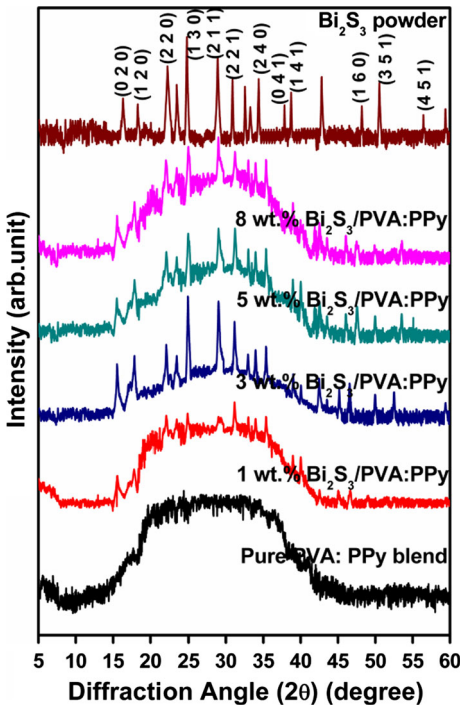

Fig. 2 X-ray diffraction patterns of pure PVA:PPy blend, Bi_2S_3 filled PVA:PPy composites and prepared Bi_2S_3 nanoparticles

matrix [8]. These peculiar changes imputed the successful incorporation and encapsulation of the Bi_2S_3 particles by the PVA:PPy blend matrix.

The crystallinity of the composites increased with the addition of Bi_2S_3 up to 3 wt%, and after that, it starts to decrease slightly. This is due to the fact that these crystalline arrangements depend on the size of the filler particles and strain within the polymer matrix [2]. The well-dispersed particles facilitate the filler-matrix interaction at the interfacial area cause the enhancement in crystallinity of the blend composite [20, 21]. At the higher Bi_2S_3 content, the agglomeration reduces the available surface area for interfacial interaction and causes the decrement in crystallinity of the composites by altering the arrangement of polymer chains at the interfacial region [22].

By obtained 2θ values, the X-ray diffraction parameters were calculated with the help of Powder-X software and also corresponding d-spacing, intensity and the area of the peaks are estimated. The interplanar spacing corresponding to Bi_2S_3-filled composites is calculated with Bragg's law $d = n\lambda/(2\sin\theta)$, where $n = 1$ is the order of reflection, θ is the Bragg's angle, and $\lambda = 1.5405$ Å is the wavelength of incident X-ray. The average inter-crystallite separation (R) [23, 24] in the composites was evaluated for crystallite peaks using the equation

$$R = \frac{5\lambda}{8\sin\theta} \quad (1)$$

The % crystallinity (X_c) was calculated using Hermans and Weidinger method as $X_c = A_c/(A_c + A_a) \times 100\%$, where A_o and A_a are the area of sharp crystalline diffraction peaks and amorphous haloes, respectively [25]. The calculated parameters are listed in Table 1.

3.2. Differential scanning calorimetry study

The DSC thermograms for pure PVA:PPy blend and Bi_2S_3-filled PVA:PPy composites are presented in Fig. 3. The glass transition temperature (T_g) is measured as a midpoint of the step changes of the endothermic curve, which decreases after the addition of Bi_2S_3 and again increased with the increase in wt% of the filler. The glass transition temperature is the temperature where the polymeric materials undergo transition involves the onset of thermally induced chain segmental motion and bond rotation. The increase in chain flexibility is the measure of an ability of a chain to rotate about the chain bonds. The lowering of T_g (73–60 °C) after the addition of Bi_2S_3 suggests that enhancement in conductivity is expected, since the lower T_g leads to easy chain relaxation in the amorphous phase of the composite and hence causes fast conduction of charges [21, 26]. The faster motion of the polymer segments is due

Table 1 X-ray diffraction parameters of pure PVA:PPy and Bi_2S_3-filled PVA:PPy composites

Amt. of Bi_2S_3 in PVA:PPy blend (wt%)	2θ (degree)	d-spacing (Å)	Inter-crystallite separation R (Å)	Crystallinity (%)
0	Amorphous			
1	15.56	5.692	7.114	56.78
	22.00	4.036	5.045	
	24.86	3.578	4.473	
	29.00	3.077	3.846	
	31.15	2.864	3.587	
	35.37	2.536	3.170	
3	15.53	5.702	7.127	77.99
	21.96	4.044	5.055	
	24.96	3.564	4.455	
	28.99	3.078	3.847	
	31.21	2.864	3.580	
	35.37	2.536	3.170	
	38.97	2.309	2.887	
	42.52	2.124	2.655	
5	15.53	5.702	7.128	72.76
	17.85	4.964	6.205	
	22.00	4.036	5.045	
	24.91	3.572	4.465	
	29.00	3.076	3.845	
	31.15	2.869	3.587	
	35.37	2.536	3.170	
	39.01	2.307	2.884	
	42.48	2.126	2.658	
	46.55	1.949	2.437	
8	15.50	5.713	7.128	66.60
	17.87	4.961	6.201	
	22.02	4.034	5.042	
	24.94	3.567	4.459	
	29.01	3.076	3.845	
	31.21	2.864	3.580	
	35.37	2.536	3.170	
	38.96	2.310	2.888	
	42.52	2.310	2.655	

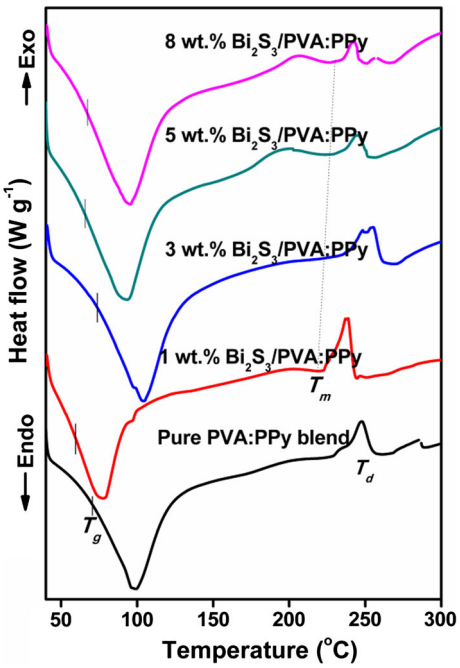

Fig. 3 DSC thermograms of pure PVA:PPy blend and Bi_2S_3-filled PVA:PPy composites

to the enhanced internal stress in the composite [27]. The increased T_g is observed at 3 wt% of Bi_2S_3, which is related to physical obstruction for the motion of polymer segments at the interface, and the variation in T_g is in obey with the XRD results. When the filler particles are incorporated into the polymer matrix, the polymer gets adsorbed on the filler surface by forming a shell. This enhances the T_g. However, with the increase in the addition of filler particles the inner structure of the composites modifies due to dense packing and the particles tends to agglomerate. The agglomeration of the particles affects the mobility of the polymer chain segments and also reduces the interfacial region and hence lowers the T_g [28, 29]. The peak corresponding to melting process is not clearly elucidated in DSC plots of all samples. However, the temperature corresponds to the melting point (217–227 °C) also follows the same behavior as that of T_g. The degradation temperature (238–254 °C) is decreased with the addition of Bi_2S_3 particles, which might be due to the interfacial interaction. The values of glass transition temperature, melting temperature and enthalpy of melting calculated as area under the melting peak are presented in Table 2.

3.3. Atomic force microscopic study

The 3-D topographical images of pure PVA:PPy blend and 3 and 8 wt% Bi_2S_3 particles-filled PVA:PPy composites are represented in Fig. 4. The valley to peak height in the AFM topography images varies from − 471 pm to 1.18 nm, − 9.88 nm to 16.6 nm and − 96.5 nm to 95.7 nm for pure PVA:PPy blend and 3 and 8 wt% Bi_2S_3-filled PVA:PPy composite, respectively. As observed in the overview, the composites exhibit a homogeneous distribution of Bi_2S_3 particles. The cluster size is also found to be increased with the increase in the concentration of bismuth sulfide particles within the polymer blend matrix. The root-mean-square (RMS) values of roughness in the area of measurement for the composites are calculated by Nanosurf software. The averaged RMS roughness for pure PVA:PPy blend, 3 wt% Bi_2S_3/PVA:PPy and 8 wt% Bi_2S_3/PVA:PPy composites are (314.22 ± 0.19) pm, (4.36 ± 0.34) nm and (28.25 ± 0.56) nm, respectively.

The clusters size is enhanced because of agglomeration, which causes the increment in surface roughness of the composites with the increase in wt% of Bi_2S_3 particles. The topography of the composites appeared to be clearer with increase in the content of Bi_2S_3 particles, due to the filling of voids present in the sample [7]. The surface topography of the Bi_2S_3-filled PVA:PPy composites suggests that the polymer blend matrix formed the envelope around the added Bi_2S_3 particles.

3.4. Scanning electron microscopy analysis

The morphology of pure PVA:PPy blend and 3 and 5 wt% Bi_2S_3-filled PVA:PPy composite films was studied by FE-SEM and is shown in Fig. 5. The surface of the pure PVA:PPy blend emerged to be rough by the presence of voids resulted by the bubbles formed during synthesis. The Bi_2S_3-filled PVA:PPy composites own highly dense matrix impute the filling of free volumes. As imputed in SEM images, the Bi_2S_3 particles are homogeneously dispersed within the polymer blend matrix. The surfaces of the composite films are highly smooth although few particles get aggregated, because of enveloping of Bi_2S_3 particles by polymer matrix which results in core–shell structure [7]. The diameters of the spheroids of the core–shell structure are calculated using PIXEL Ruler and are found to be in the range 218–900 nm. The increment in the number of particles and their regular distribution within the polymer matrix is observed in SEM images.

3.5. Mechanical properties

The homogeneity of filler in the composites and the stronger interfacial interaction between nanofillers and the polymer matrix have a significant influence on the mechanical properties [30]. The behavior of the stress and applied strain for the prepared polymer composites is represented in Fig. 6. The mechanical parameters obtained in the measurement are tabulated in Table 3. At the lower strain, the stress in the composite strip increased linearly

Table 2 Glass transition temperature, melting temperature, degradation temperature and enthalpy of melting for pure PVA:PPy and Bi_2S_3-filled PVA:PPy composites

Amount of Bi_2S_3 in PVA:PPy blend (wt%)	T_g (°C)	T_m (°C)	T_d (°C)	ΔH_m (J g^{-1})
0	70.41	–	254.04	–
1	60.01	217.00	238.92	15.55
3	72.88	–	247.14	–
5	65.62	225.22	244.40	60.23
8	66.33	227.06	243.08	27.79

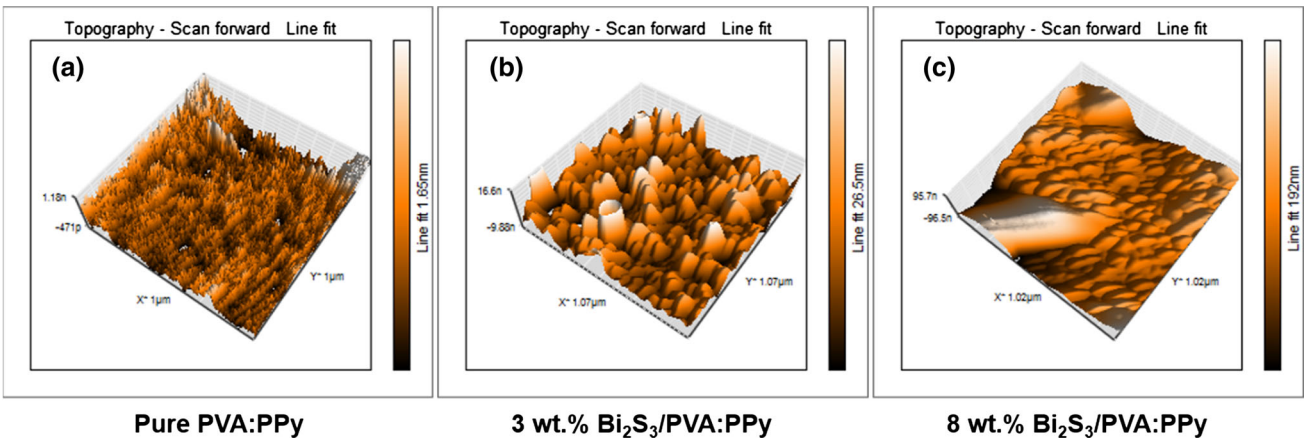

Fig. 4 3-D topographical images of (**a**) pure PVA:PPy blend, (**b**) 3 wt% and (**c**) 8 wt% Bi_2S_3 particles-filled PVA:PPy composites

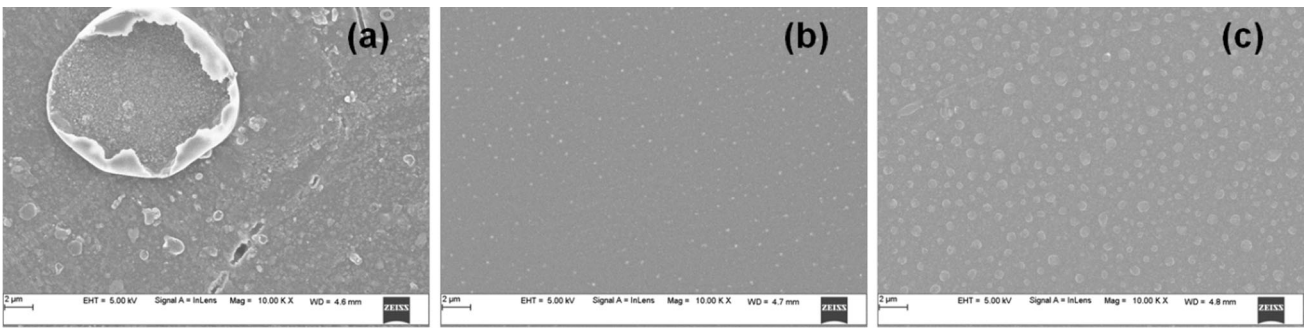

Fig. 5 FE-SEM images of (**a**) pure PVA:PPy blend, (**b**) 3 wt% Bi_2S_3/PVA:PPy composite, (**c**) 5 wt% Bi_2S_3/PVA:PPy composite

and this property is called elasticity. But after a certain strain, the stress in the composite material remains uniform and does not follow linearity, and the behavior is called plasticity. It is noted that Young's modulus, toughness and % elongation at fracture get enhanced with the increase in wt% of bismuth sulfide in PVA:PPy blend and exhibit their maximum for 5 wt% Bi_2S_3-filled PVA:PPy blend composite, which imputes the increased elastic nature of the composite caused by the improved interfacial interaction and also considerably high crystallinity [19].

The mechanical parameters are decreased for 8 wt% Bi_2S_3 because the presence of more free volume restricts the load transfer between the polymer matrix and additive particles, which is also supported by PALS data [31]. The values of the % elongation at fracture are small compared to the literature, implied that the samples are less ductile. The tensile strength decreased suddenly after the addition of Bi_2S_3, and the results are in agreement with the reported literature [32]. The toughness of the material is estimated as the area under the stress–strain curve, which gives the energy absorbed by the composite before getting a fracture. Among the prepared polymer blend composites, 5 wt% Bi_2S_3/PVA:PPy blend composite is highly tough one.

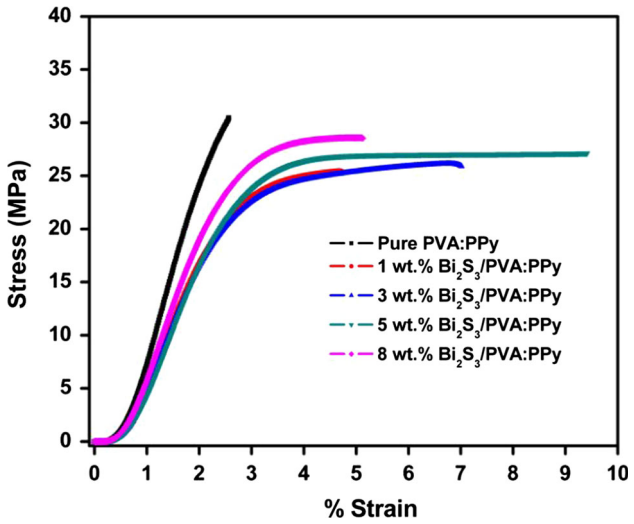

Fig. 6 Stress–strain curves for pure PVA:PPy and Bi_2S_3/PVA:PPy composites

3.6. Electrical conductivity

The electrical conductivity of the Bi_2S_3 particles-filled PVA:PPy composites is obtained by the impedance spectroscopy. The typical Cole–Cole plots for pure PVA:PPy blend and Bi_2S_3 particles-filled PVA:PPy nanocomposites at room temperature are given in Fig. 7(a). The Cole–Cole plots consist of the imaginary component of the impedance (Z'') plotted against the real component (Z') which illustrates the frequency response of the electrode/electrolyte system. In the present case, the complex impedance plots are characterized by the presence of a semicircle followed by a spike. The semicircle formed at the high-frequency region is assigned to bulk conductivity, and the linear region in low-frequency range is attributed to the polarization at the electrode [23]. The straight line is nearly around 45° with real impedance axis, implying that the polymer nanocomposite films can act as capacitors. The decentralization of semicircles from the X-axis suggesting the presence of non-Debye relaxation process in the composites due to interfacial charge transfer and hence the material follows Cole–Cole formalism [33].

The data obtained experimentally in impedance analyzer are fitted by using the Z-SimpWin software. The best fit for all the prepared composites is obtained when employing an equivalent circuit consists of serial and parallel combinations of resistance (R) and capacitance (C) coupled with a Warburg element (W), and the equivalent circuit is depicted in Fig. 7(b). In the equivalent circuit, R_s corresponds to the contact resistance of the sample and the electrode and is obtained as the shift of the impedance plot from the origin along the real Z' axis. Meanwhile, a Warburg element (W) corresponds to a straight line at low

Table 3 Mechanical parameters of pure PVA:PPy and Bi_2S_3/PVA:PPy composites

Amount of Bi_2S_3 in PVA:PPy blend (wt%)	Young's modulus (MPa)	Tensile strength (MPa)	Elongation at fracture (%)	Toughness (J mm^{-3})
0	1081.41 ± 0.86	30.182 ± 0.68	2.56 ± 0.07	33.60 ± 0.62
1	968.52 ± 1.25	25.13 ± 0.92	4.71 ± 0.05	75.07 ± 0.82
3	959.54 ± 1.02	26.92 ± 0.36	7.01 ± 0.06	133.04 ± 1.3
5	976.16 ± 0.95	28.44 ± 0.42	9.41 ± 0.04	203.52 ± 2.6
8	990.30 ± 1.30	26.55 ± 0.82	5.12 ± 0.01	96.64 ± 0.85

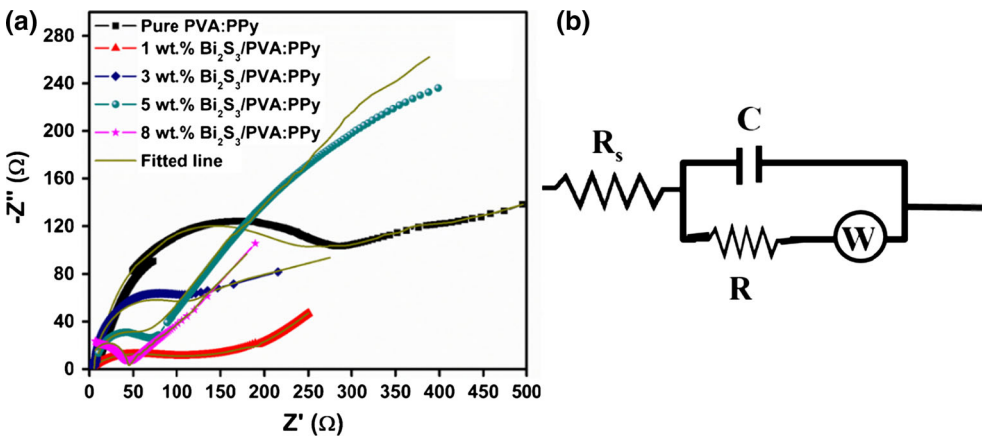

Fig. 7 (**a**) Typical Cole–Cole plots, (**b**) Equivalent circuit for fitting the impedance data of pure PVA:PPy blend and Bi_2S_3 particles-filled PVA:PPy nanocomposites at room temperature

frequencies due to the diffusion-limiting process at the electrode–electrolyte interface [34]. The extracted parameters for the circuit elements obtained after fitting the impedance data of pure PVA:PPy blend and Bi_2S_3 particles-filled PVA:PPy composites at room temperature are collected in Table 4.

The bulk conductivity (σ) of composite films is calculated using the obtained bulk resistance R in the plot after equivalent circuit fitting.

$$\sigma = \frac{t}{RA} \tag{2}$$

where A is the electrode–electrolyte contact area and t is the thickness of the composite film. Compared to the solid polymer electrolyte without fillers, an appreciable reduction in the bulk resistance is observed in the Bi_2S_3-filled composite electrolytic films. Hence, the enhanced conductivity is detected in all Bi_2S_3-filled PVA:PPy composites. The composite 8 wt% Bi_2S_3 filled PVA:PPy blend displayed the highest conductivity of 1.06×10^{-3} S cm^{-1} at room temperature, which is slightly higher than that of 5 wt% Bi_2S_3/PVA:PPy. The rate of increase in conductivity is reduced at the higher loading of the filler, which might be due to the aggregation of the filler particles. The enhancement in conductivity after the addition of Bi_2S_3 particles is due to the increased conducting pathways raised by the encapsulation of filler particles by the conducting polymer blend matrix [16, 25].

3.7. Positron annihilation lifetime studies

The positron annihilation lifetime spectroscopic measurements were taken in order to recognize the effect of Bi_2S_3 filler on the microstructure of PVA:PPy composites. The microstructural modifications related to free volumes of the polymeric material are used to control the molecular packaging and in turn the bulk properties [11]. The lifetime spectrum resulted by the positron annihilation within the present composites possesses three components. τ_1 corresponds to the free annihilation, τ_2 represents the lifetime of the positrons trapped in the defects present in the crystalline–amorphous interface region, and τ_3 is the lifetime corresponding to the o-Ps pick-off annihilation in the free volumes of the polymeric material. τ_3 is related to free volume hole radius by the model developed on the basis of theoretical models originally proposed by Tao and Eldrup [35, 36]. In this model, positronium is assumed to be localized in a spherical potential well having an infinite potential barrier of radius R_o with an electron layer in the region $R < r < R_o$. The semiempirical relation between o-Ps lifetime τ_3 and the radius of the free volume cavity R in polymers is given by the equation

$$\tau_3 = \frac{1}{2}\left[1 - \frac{R}{R_o} + \frac{1}{2\pi}\sin\left(\frac{2\pi R}{R_o}\right)\right]^{-1} \quad \text{ns} \tag{3}$$

where $R_o = R + \Delta R$, where $\Delta R = 1.657$ Å is an empirical parameter representing the electron layer thickness derived from the observed o-Ps lifetimes in molecular solids (polymers & zeolites) [10, 37]. The o-Ps lifetime and intensity (τ_3 and I_3) are related to size and content of free volumes, respectively. The average size of the free volume (V_f) [38] is given by

$$V_f = \left(\frac{4}{3}\right)\pi R \tag{4}$$

From the measured free volume size, fractional free volume can be determined by the equation

$$F_v = AV_fI_3 \tag{5}$$

where A is a structural constant which is an arbitrarily chosen scaling factor for a spherical cavity and estimated as 0.0018 Å^3 from different experiments [16, 39].

The free volume parameters for Bi_2S_3 particles-filled PVA:PPy composites derived from the PATFITT program and using formulas are listed in Table 5. The variation of an o-Ps lifetime (τ_3), o-Ps intensity (I_3), free volume size (V_f) and fractional free volume (F_v) in PVA:PPy blend with different amount of Bi_2S_3 particles addition is shown in Fig. 8. The o-Ps lifetime (τ_3) and free volume size (V_f) showed a slightly lesser value with the incorporation of 1 wt% of Bi_2S_3 particles into PVA:PPy blend, and thereafter o-Ps lifetime (τ_3) increased with the increase in filler concentration. At the lower wt% of Bi_2S_3 filler loading, the particles got easily dispersed in the polymer matrix and restricted the polymer chain mobility and hence free volume hole size reduced due to the formation of interfaces [13, 16]. The increased filler content enhanced the interfacial sites results in larger interfaces, and also the arrangement of polymer chain near the interface of fillers is interrupted due to agglomeration of Bi_2S_3 nanoparticles [16], indicated by increasing τ_3 and V_f with the wt% of Bi_2S_3. The initial constraints for the motion of polymer chains are reduced at the higher loading; this consequence is consistent with the variation of T_g as observed in DSC results [27, 39].

The free volume content represented by the o-Ps intensity I_3 shows no change in the initial concentration of Bi_2S_3 and decreased above 3 wt% of Bi_2S_3 in PVA:PPy blend. This is due to the reduction in a number of voids available for o-Ps annihilation due to the aggregation of Bi_2S_3 particles [40]. The inhibition of o-Ps formation due to the agglomeration of nanoparticles cannot be ruled out [25, 41]. The overall change in the free volume represented by the fractional free volume (F_v) is decreased at the lower amount of filler loading because of the occupation of the

Table 4 The values fitting parameters for pure PVA:PPy blend and Bi_2S_3-filled PVA:PPy composites at room temperature calculated from equivalent circuit model

Sample	C (μF)	R (Ω)	W ($s^{1/2}$ Ω^{-1} cm^{-2})	Conductivity (S cm^{-1})
Pure PVA:PPy	1.33	250	4.99×10^{-4}	1.02×10^{-4}
1 wt% Bi_2S_3/PVA:PPy	0.013	99	1.32×10^{-4}	2.42×10^{-4}
3 wt% Bi_2S_3/PVA:PPy	2.74	95	7.80×10^{-4}	2.60×10^{-4}
5 wt% Bi_2S_3/PVA:PPy	0.015	49	7.04×10^{-5}	9.61×10^{-4}
8 wt% Bi_2S_3/PVA:PPy	0.017	43	5.94×10^{-4}	1.06×10^{-3}

Table 5 Free volume parameters obtained by positron lifetime annihilation spectroscopy results

Sample	τ_3 (ns)	I_3 (%)	V_f (Å^3)	F_v (%)
Pure PVA:PPy	2.31 ± 0.027	8.80 ± 0.145	127.82 ± 2.58	2.024 ± 0.036
1 wt% Bi_2S_3/PVA:PPy	2.27 ± 0.026	8.74 ± 0.145	123.81 ± 2.45	1.947 ± 0.036
3 wt% Bi_2S_3/PVA:PPy	2.38 ± 0.028	8.76 ± 0.142	134.94 ± 2.74	2.127 ± 0.036
5 wt% Bi_2S_3/PVA:PPy	2.44 ± 0.025	8.66 ± 0.141	141.14 ± 2.50	2.200 ± 0.033
8 wt% Bi_2S_3/PVA:PPy	2.48 ± 0.027	8.28 ± 0.142	145.24 ± 2.73	2.165 ± 0.035

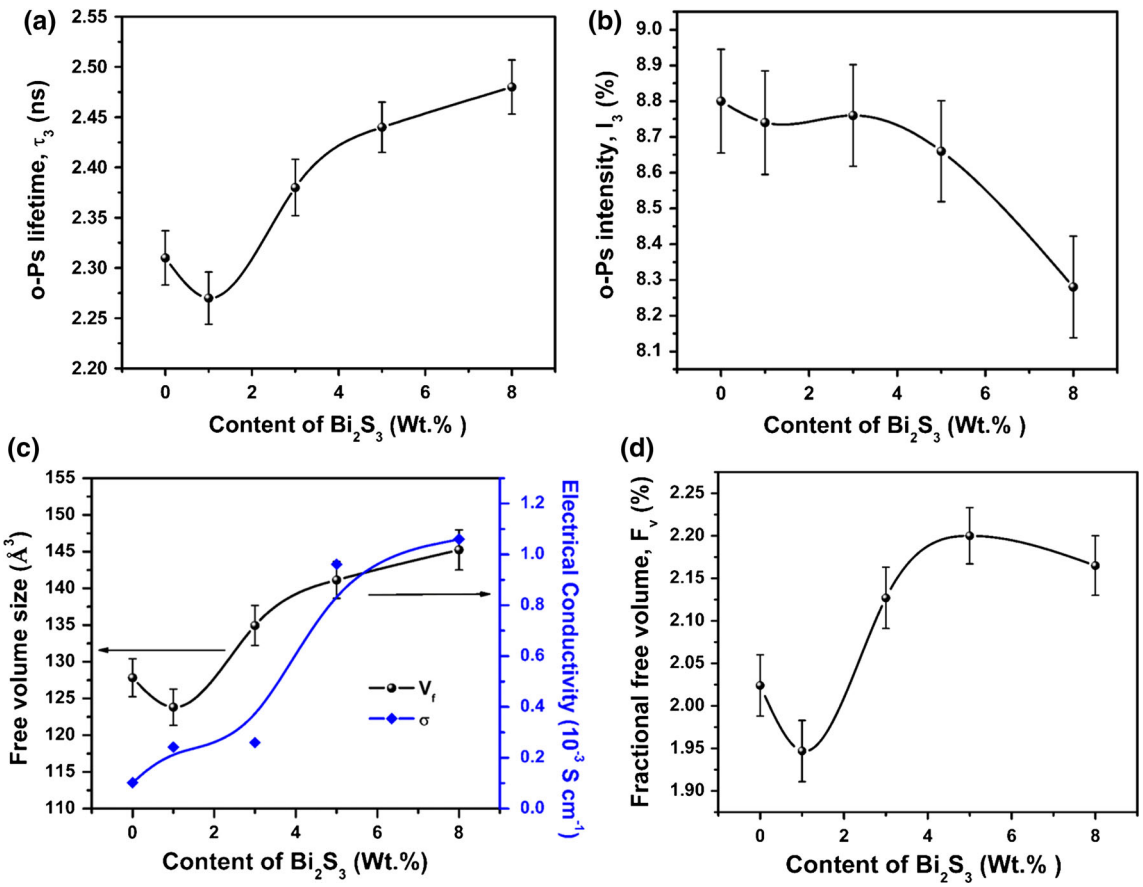

Fig. 8 The variation of (**a**) o-Ps lifetime (τ_3), (**b**) o-Ps intensity (I_3), (**c**) free volume size (V_f) and electrical conductivity (σ) and (**d**) fractional free volume (F_v) with different amounts of Bi_2S_3 particles in PVA:PPy

Bi_2S_3 particles. Above 5 wt% of Bi_2S_3 addition, it rises abruptly due to the increased amorphous phase by the contribution of interfaces and hence results in enhanced conductivity [25]. The variation in o-Ps intensity, free volume size and free volume fraction support the variation in the crystallinity of the samples with the addition of filler as observed in XRD studies.

The variation in free volume size and electrical conductivity with the addition of Bi_2S_3 particles is shown in Fig. 7(c). The conductivity of nanofiller-added composites depends on the microstructural factors such as the geometry of the particles, aspect ratio, dispersion, and filler–filler as well as filler–matrix interaction. Even though the agglomeration of nanoparticles occurs with the increase in filler content in the polymer blend matrix, the number density of mobile charge carriers increased and also the formation of conducting network at the interface facilitated. This leads to the enhancement in electrical conductivity [16] with the increased addition of Bi_2S_3 particles. Moreover, the increased interfacial width provides more space for charge carriers mobility and hence the enhancement in conductivity is attained [38, 42].

4. Conclusions

The present study has provided the comprehensive picture of the effect of the addition of Bi_2S_3 particles on the microstructural, thermal, mechanical and electrical properties of PVA:PPy blend, where the composite films with different contents of dispersed Bi_2S_3 were prepared using a simple aqueous solution casting method. As observed in XRD analysis, the crystallinity increased at the lower loading of Bi_2S_3 content and then decreased after 3 wt% addition due to interfacial interaction. DSC studies depicted that the variation in the molecular packing caused the variation in thermal properties of the composites. The AFM and SEM records imputed the filling of voids in the PVA:PPy blend matrix along with the aggregate formation at the higher loading and the encapsulation of the polymer matrix around the filler particles. The improved mechanical properties in 5 wt% Bi_2S_3/PVA:PPy composite are resulted from the interfacial interaction as well as crystallinity. The electrical conductivity obtained by Cole–Cole fitting is maximum in 8 wt% Bi_2S_3/PVA:PPy blend at room temperature due to the encapsulation of Bi_2S_3 particles by the polymer blend matrix and increased conductive network. The positron annihilation lifetime parameters viz., o-Ps lifetime, o-Ps intensity and free volume hole size altered remarkably by the incorporation of Bi_2S_3 nanofillers. The variation in the free volume characteristics because of interfacial interaction is considered to correlate with structural, thermal and electrical properties of the composites.

Acknowledgements One of the authors, Vidyashree Hebbar is thankful to Karnatak University, Dharwad, for awarding UGC-UPE fellowship (KU/Sch/UGC-UPE/2014-15/890). The authors also thank the UGC, New Delhi, for the SAP-CAS Phase-II (F.530/9/CAS-II/2015(SAP-I) for providing research grants, and Science and Engineering Research Board (SERB), Department of Science and Technology (DST), Government of India, for the research projects (SR/FTP/PS-011/2010), (SB/EMEQ-089/2013) and (SB/EMEQ-213/2014). The authors would like to acknowledge USIC, Karnatak University, Dharwad, for DSC and AFM facilities. The authors would further acknowledge MIT, Manipal, for XRD measurement facility.

References

[1] J Liu, Y Luo, Y Wang, Y Deng and X Xie *Rsc Adv.* **5** 96258 (2015)
[2] M T Ramesan *Polym. - Plast. Technol. Eng.* **51** 1223 (2012)
[3] N Romyen, S Thongyai, P Praserthdam and G A Sotzing *J. Mater. Sci. Mater. Electron.* **24** 2897 (2013)
[4] E F De Melo, K G B Alves, S A Junior and C P De Melo *J. Mater. Sci.* **48** 3652 (2013)
[5] W Yin, H Liu and L H Gan *J. Appl. Polym. Sci.* **72** 95 (1999)
[6] W Sun et al. *J. Power Sources* **309** 135 (2016)
[7] V Hebbar and R F Bhajantri *Mater. Sci. Eng. B* **224** 171 (2017)
[8] P Hazra, A Jana, M Hazra and J Datta *Rsc Adv.* **4** 33662 (2014)
[9] Y Wang, K F Cai and X Yao *J. Nanoparticle Res.* **14** 848 (2012)
[10] M Mukherjee, D Chakravorty and P M G Nambissan *Phys. Rev. B* **57** 848 (1998)
[11] R Xia et al. *Phys. Chem. Chem. Phys.* **3616** 3616 (2017)
[12] J C Machado, G G Silva and L S Soares *J. Polym. Sci. Part B Polym. Phys.* **38** 1045 (2000)
[13] G Xue, J Zhong, S Gao and B Wang *Carbon* **96** 871 (2016)
[14] C Basavaraja, P X Thinh, W J Kim, M Revanasiddappa and D S Huh *Polym. Compos.* **33** 1534 (2012)
[15] T Sheela et al. *J. Non. Cryst. Solids* **454** 19 (2016)
[16] S Ningaraju and H B Ravikumar *J. Polym. Res.* **24** 11 (2017)
[17] K H Kate, K Singh and P K Khanna *Synth. React. Inorganic, Met. Nano-Metal Chem.* **41** 199 (2011)
[18] Z-H Ge, B-P Zhang, Z-X Yu and B-B Jiang *Crystengcomm.* **14** 2283 (2012)
[19] S K Sharma et al. *Phys. Chem. Chem. Phys.* **16** 1399 (2014)
[20] P Bala, B K Samantaray, S K Srivastava and G B Nando *J. Appl. Polym. Sci.* **92** 3583 (2004)
[21] S Ibrahim and M R Johan *Int. J. Electrochem. Sci.* **7** 2596 (2012)
[22] S K Sharma, J Prakash, K Sudarshan, P Maheshwari, D Sathiyamoorthy and P K Pujari *Phys. Chem. Chem. Phys.* **14** 10972 (2012)
[23] V Hebbar, R F Bhajantri and J Naik *J. Mater. Sci. Mater. Electron.* **28** 5827 (2017)
[24] P P Kundu, J Biswas, H Kim and S Choe *Eur. Polym. J.* **39** 1585 (2003)
[25] R F Bhajantri, V Ravindrachary, A Harisha, C Ranganathaiah and G N Kumaraswamy *Appl. Phys. A* **87** 797 (2007)
[26] D K Pradhan, B K Samantaray, R N P Choudhary, N K Karan, R Thomas and R S Katiyar *Int. J. Electrochem. Sci.* **2** 861 (2007)
[27] S K Sharma, K Sudarshan, M Sahu and P K Pujari (2016) *Rsc Adv.* **6** 67997
[28] A Dorigato, Y Dzenis and A Pegoretti *Mech. Mater.* **61** 79 (2013)

[29] B Qi, S R Lu, X E Xiao, L L Pan, F Z Tan and J H Yu, *eXPRESS Polym. Lett.* **8** 467 (2014)
[30] X Zhao, Q Zhang, D Chen and P Lu (2010) *Macromolecules* **43** 2357
[31] S K Sharma, J Prakash and P K Pujari *Phys. Chem. Chem. Phys.* **17** 29201 (2015)
[32] Y Chen, Y Qi, Z Tai, X Yan, F Zhu and Q. Xue *Eur. Polym. J.* **48** 1026 (2012)
[33] M Sassi, A Oueslati and M Gargouri *Appl. Phys. A* **119** 763 (2015)
[34] W Liu et al. *Nano Lett.* **15** 2740 (2015)
[35] S J Tao *J. Chem. Phys.* **56** 5499 (1972)
[36] M Eldrup, D Lightbody and J N Sherwood *Chem. Phys.* **63** 51 (1981)
[37] V Ravindrachary, R F Bhajantri, A Harisha, Ismayil and C Ranganathaiah *Phys. Status Solidi C* **6** 2438 (2009)
[38] S D Praveena, V Ravindrachary and R F Bhajantri *Polym. Compos.* **35** 1267 (2014)
[39] U Rana, P M G Nambissan, S Malik and K Chakrabarti, *Phys. Chem. Chem. Phys.* **16** 3292 (2014)
[40] G Dlubek, M A Alam, M Stolp and H-J Radusch *J. Polym. Sci. Part B Polym. Phys.* **37** 1749 (1999)
[41] R F Bhajantri, V Ravindrachary, A Harisha, Ismayil and C Ranganathaiah *Phys. Status Solidi C* **6**, 2429 (2009)
[42] K V Aneesh Kumar, S Krishnaveni, P M G Nambissan, C Ranganathaiah and H B Ravikumar *J. Non. Cryst. Solids* **471** 151 (2017)